THE JOURNAL OF BIOLOGICAL CHEMISTRY VOL. 283, NO. 42, pp. 28563–28573, October 17, 2008

A Central Role for CK1 in Catalyzing Phosphorylation of the p53 Transactivation Domain at Serine 20 after HHV-6B Viral Infection*

Received for publication, June 9, 2008, and in revised form, July 29, 2008 Published, JBC Papers in Press, July 31, 2008, DOI 10.1074/jbc.M804433200

Nicola J. MacLaine[‡], Bodil Øster[§], Bettina Bundgaard[§], Jennifer A. Fraser[‡], Carolyn Buckner[‡1], Pedro A. Lazo[¶], David W. Meek[‖], Per Höllsberg[§2], and Ted R. Hupp[‡3]

From the Institute of Genetics and Molecular Medicine, Division of Cancer Biology, CRUK p53 Signal Transduction Group, [‡]University of Edinburgh, Crewe Road South, Edinburgh, EH4 2XR, United Kingdom, the [§]Institute of Medical Microbiology and Immunology, University of Aarhus, Aarhus DK 800, Denmark, [¶]Programa de Oncología Translacional, Instituto de Biología Molecular y Celular del Cáncer, Centro de Investigación del Cáncer, Consejo Superior de Investigaciones Científicas, Universidad de Salamanca, Salamanca 37071, Spain, and [‖]Biomedical Research Centre, Ninewells Hospital and Medical School, University of Dundee, Dundee DD1 4HN, United Kingdom

The tumor suppressor protein p53 is activated by distinct cellular stresses including radiation, hypoxia, type I interferon, and DNA/RNA virus infection. The transactivation domain of p53 contains a phosphorylation site at Ser^{20} whose modification stabilizes the binding of the transcriptional co-activator p300 and whose mutation in murine transgenics induces B-cell lymphoma. Although the checkpoint kinase CHK2 is implicated in promoting Ser^{20} site phosphorylation after irradiation, the enzyme that triggers this phosphorylation after DNA viral infection is undefined. Using human herpesvirus 6B (HHV-6B) as a virus that induces Ser^{20} site phosphorylation of p53 in T-cells, we sought to identify the kinase responsible for this virus-induced p53 modification. The p53 Ser^{20} kinase was fractionated and purified using cation, anion, and dye-ligand exchange chromatography. Mass spectrometry identified casein kinase 1 (CK1) and vaccinia-related kinase 1 (VRK1) as enzymes that co-eluted with virus-induced Ser^{20} site kinase activity. Immunodepletion of CK1 but not VRK1 removed the kinase activity from the peak fraction, and bacterially expressed CK1 exhibited Ser^{20} site kinase activity equivalent to that of the virus-induced native CK1. CK1 modified p53 in a docking-dependent manner, which is similar to other known Ser^{20} site p53 kinases. Low levels of the CK1 inhibitor D4476 selectively inhibited HHV-6B-induced Ser^{20} site phosphorylation of p53. However, x-ray-induced Ser^{20} site phosphorylation of p53 was not blocked by D4476. These data highlight a central role for CK1 as the Ser^{20} site kinase for p53 in DNA virus-infected cells but also suggest that distinct stresses may selectively trigger different protein kinases to modify the transactivation domain of p53 at Ser^{20}.

The tumor suppressor protein p53 is a key player in the survival or death decision that cells face after exposure to a variety of metabolic and genotoxic stresses (1). The transient accumulation and activation of p53 in response to various cellular stresses enables the protein to modulate the expression of numerous genes involved in cell cycle arrest, DNA repair, and/or apoptosis. The initiation of either transient cell cycle arrest and damage repair or apoptosis is dependent on the cell and damage type, the severity of damage, and the cellular microenvironment. Phosphorylation and acetylation events that control interactions between the transcription factor p53 and its negative regulators (Mdm2, COP1, and Pirh2) or co-activators (p300) are ultimately involved in modulating p53-dependent gene expression in response to cellular stress (2). In particular, phosphorylation at Thr^{18} within the N-terminal conserved *BOX-I* domain of p53 blocks the binding of Mdm2, whereas phosphorylation at Ser^{20}, also within the *BOX-I* domain, enables the binding of p300 (3–5). Thus, phosphorylation in this transactivation domain serves to stimulate rather than inhibit p53 function. In addition, phosphorylation at Ser^{392} within the C terminus of p53 stimulates the sequence-specific DNA-binding function of p53 (6).

The generation of transgenic mice with phosphoacceptor site mutations (to alanine) at the key regulatory phosphoacceptor sites of Ser^{20} and Ser^{392} equivalents in murine p53 results in elevated cancer incidence. Mutation of Ser^{20} results in enhanced spontaneous B-cell lymphoma and attenuated damage-induced apoptosis in B-cells (7), whereas mutation of Ser^{392} results in enhanced UV-induced skin cancer or carcinogen-induced bladder cancer (8, 9). These biochemical and genetic results highlight the critical role that phosphorylation of p53 can play in modulating its tumor suppressor function and the likelihood that these phosphorylation events are "stress-" and/or cell type-specific. Presumably, the use of transgenic phosphomutated systems will further uncover the cell- and stress-specific function of these multiple covalent modifications.

Although members of the calcium calmodulin kinase superfamily, particularly the checkpoint kinases 1 and 2 (CHK1 and CHK2) and death-associated protein kinase 1 (DAPK-1), are

* The costs of publication of this article were defrayed in part by the payment of page charges. This article must therefore be hereby marked "*advertisement*" in accordance with 18 U.S.C. Section 1734 solely to indicate this fact.
[1] Supported by the Biotechnology and Biological Sciences Research Council-Radical Solutions for Researching the Proteome (RASOR) Interdisciplinary Research Collaboration in Proteomic Technologies.
[2] Supported by grants from the Lundbeck Foundation, Edith Stern, and the Faculty of Health Science (Program on Molecular Medicine), University of Aarhus, Denmark.
[3] Supported by Cancer Research UK. To whom correspondence should be addressed. Tel.: 44-1317773538; Fax: 44-1317773583; E-mail: ted.hupp@ed.ac.uk.

genetic activators of the p53 pathway, other kinases have also been shown to phosphorylate and activate p53. For example, vaccinia-related kinase 1 (VRK1) and casein kinase 1 (CK1) have been reported to phosphorylate p53 at Thr^{18} (10), although the latter requires prior phosphorylation of p53 at Ser^{15} (11). Controversy remains as to which kinases are most important for the activation of p53 in response to distinct cellular stress. It is possible that the exact kinase(s) involved and the residue(s) modified are specific to both the cell and damage type, which would explain the slight disparities in the results reported to date, and provide a mechanism for a context-based cellular survival *versus* death decision to be made. Nevertheless, the identification and characterization of the kinases involved in the phosphorylation of p53 are essential to the further elucidation of the regulation of p53.

In addition to the well established activation of p53 by ionizing and nonionizing radiation, anoxia, hypoxia, and type I interferons, more recent research has shown that DNA and RNA viruses can activate the p53 response (12, 13). It has been previously shown that human herpesvirus 6B (HHV-6B) infection of HCT116 and MOLT-3 cancer cell lines induced p53 phosphorylation (at Ser^{15}, Ser^{20}, Ser^{33}, and Ser^{392}) and p53 accumulation in both nuclear and cytoplasmic fractions (14, 15). It has also been shown that HHV-6B-infected cells were mostly nonapoptotic, and it has been suggested that in this context, p53 phosphorylation and accumulation may act as a survival factor rather than cell death inducer. Thus, p53 is a central sensor of both DNA damage and immune system perturbation. The DNA virus-induced stress provides a novel model to examine the kinases that target the Ser^{20} site of p53.

The aim of this study was to identify the p53 Ser^{20} kinase that is activated after HHV-6B infection of MOLT-3 cells and to investigate whether the Ser^{20} kinase operates in a dual site docking-dependent manner, like members of the calcium calmodulin kinase superfamily. We show that the enzyme responsible for this virus-induced phosphorylation of p53 is the DNA damage-regulatory enzyme CK1. These data suggest a dominant role for CK1 in p53 activation after HHV-6B virus infection and highlight a specific kinase pathway for further integration into the antiviral sensing machinery of the cell.

EXPERIMENTAL PROCEDURES

Chemicals, Reagents, Recombinant Proteins, and Antibodies—All reagents were purchased from Sigma unless otherwise stated. The CK1 inhibitor D4476 was purchased from Merck. Overlapping synthetic 15-mer biotinylated peptides from the coding sequence of human p53 (see Table 1) (Mimotopes, Melbourne, Australia) were resuspended in DMSO to a concentration of 10 mM. Full-length p53 (FLp53)[4] tetramers, recombinant DAPK-1 core domain, and recombinant GST-CK1δ kinase domain were purified as described previously (3, 11, 18). DO-1 and DO-12 antibodies to p53 were kindly provided by B. Vojtesek (Masaryk Memorial Cancer Institute, Brno, Czech Republic). Antibodies to p53 phosphorylated at Thr^{18} (P-p53 Thr^{18}) and Ser^{392} (P-p53 Ser^{392}) were described previously (16). 1F6 and VC1 antibodies to VRK1 were generated as described previously (17). P-p53 Ser^{15} antibody to p53 phosphorylated at Ser^{15} and an antibody against CK1 were purchased from Cell Signaling Technology (supplied by New England Biolabs, Hitchin, UK). P-p53 Ser^{20} antibody to p53 phosphorylated at Ser^{20} and antibodies against CK1α, CHK1, and CHK2 were obtained from Santa Cruz Biotechnology, Inc. (Santa Cruz, CA) (supplied by Insight Biotechnology, Wembley, UK). Antibodies to AMPKα1, AMPKα2, and CK2 were purchased from Upstate (Millipore, Watford, UK); an antibody to DAPK-1 was from BD Biosciences (Oxford, UK); and antibodies to DAPK-2 and DAPK-3 were from Abcam (Cambridge, UK). Rabbit anti-mouse or swine anti-rabbit secondary antibodies were obtained from Dako (Ely, UK), and donkey anti-goat secondary antibody was purchased from Santa Cruz Biotechnology.

Purification of the p53 Ser^{20} Kinase—The human T-cell acute lymphoblastic leukemia cell line, MOLT-3, was infected with HHV-6B strain PL-1 as previously described (14). High salt extracts were prepared from MOLT-3 cells infected with or without HHV-6B for 48 h. Briefly, cells were lysed in 20 mM Tris-HCl (pH 7.5), 0.5 M NaCl, 1 mM Na_2EDTA, 1 mM EGTA, 1% (v/v) Triton X-100, 2.5 mM $Na_4P_2O_7$, 1 mM β-glycerophosphate, 1 mM Na_3VO_4, and 1 μg/ml leupeptin. Lysates were treated with Benzonase nuclease (Merck), syringed, and collected after centrifugation at 12,000 rpm for 5 min at 4 °C. Fractionation of kinase activity from high salt lysates was performed using a Q-Sepharose Fast Flow anion exchanger with a linear gradient of 0–1 M KCl in a 10-column volume of 20 mM HEPES (pH 8.0), 10% (v/v) glycerol, 1 mM dithiothreitol (DTT), 1 mM benzamidine, and protease inhibitor mixture tablets (Roche Applied Science). The flow-through and 42 12-ml fractions were collected and assayed for their *in vitro* kinase activity toward FLp53 tetramers (see below), and positive fractions were pooled. Further fractionation of kinase activity from the positive fractions was performed using a Reactive Brown 10-agarose cation exchanger with a linear gradient of 10 mM to 2 M KCl in a 20-column volume of 25 mM HEPES (pH 7.5), 10% (v/v) glycerol, 0.02% (v/v) Triton X-100, 1 mM DTT, 1 mM benzamidine, and protease inhibitor mixture tablets. Flow-through and 77 1.3-ml fractions were collected and assayed as above, and positive fractions were pooled. A final fractionation of kinase activity was performed using a HiTrap SP-Sepharose HP cation exchanger (GE Healthcare) with a linear gradient of 10 mM to 2 M KCl in a 20-column volume of 25 mM HEPES (pH 7.5), 10% (v/v) glycerol, 0.02% (v/v) Triton X-100, 1 mM DTT, 1 mM benzamidine, and protease inhibitor mixture tablets. The flow-through and 100 1-ml fractions were collected and assayed as above.

In Vitro Kinase Assays—FLp53 tetramer *in vitro* kinase assays were described previously (18). Briefly, the kinase source (0.2–2 μl of lysate or fraction or flow-through, 0.2 μl of DAPK-1 core domain, or 1 μl of recombinant GST-CK1δ) was incubated with p53 substrate (100 ng of FLp53 tetramers) in a 20-μl reaction volume containing 25 mM HEPES (pH 7.5), 25 mM KCl, 1 mM $MgCl_2$, 20 μM EDTA, 0.1 mM DTT, and 0.1 mM ATP. Reaction mixtures were incubated at 30 °C for 45 min, and reactions were

[4] The abbreviations used are: FLp53, full-length p53; GST, glutathione *S*-transferase; P-p53, phosphorylated p53; DTT, dithiothreitol; bis-tris, 2-[bis(2-hydroxyethyl)amino]-2-(hydroxymethyl)propane-1,3-diol; MS, mass spectrometry; MS/MS, tandem mass spectrometry.

terminated by the addition of 30 μl of SDS sample buffer containing 0.2 M DTT. Peptide kinase assays were performed by incubating p53 peptide fragments with the above described kinase reaction mixtures for 20 min at room temperature prior to the addition of the kinase source. p53 peptides fragments were added to a final concentration of 200 μM. Negative control reactions, lacking either the kinase source or the kinase substrate were included, along with DMSO solvent controls for peptide kinase assays.

CK1 Inhibitor Experiments—Mock-infected and HHV-6B-infected MOLT-3 cells were treated with 10–100 μM CK1 inhibitor D4476, concomitantly with infection, for 48 h. Alternatively, MOLT-3 cells were pretreated with 10–60 μM D4476 for 44 h before exposure (or sham exposure) to a 6-gray x-ray and further culture for 4 h. DMSO solvent controls were included, and cells were lysed as described previously (15).

Western Blotting—Lysates, flow-through, fractions, eluates, or kinase assay samples (10 μl) were resolved by SDS-PAGE through 10% (w/v) Tris-glycine gels and transferred onto nitrocellulose membranes (Hybond ECL; GE Healthcare). Membranes were probed with primary antibodies, followed by secondary antibodies conjugated to horseradish peroxidase. Bound antibody was detected by ECL.

Mass Spectrometry—Fractions from the HiTrap SP-Sepharose HP cation exchanger column (1 ml each) were concentrated ~25-fold using Centricon YM10 centrifugal devices (Millipore). Flow-through and fractions (10 μl) were resolved by SDS-PAGE through a 4–12% (w/v) bis-tris gel (Invitrogen) and stained with colloidal blue (Invitrogen). Proteins enriched in the peak fraction (fraction 31) were excised from the gel, protein in-gel digestions were performed with 0.1 pmol/μl trypsin gold (Promega, Southampton, UK), and extracted peptides were resuspended in 2% (v/v) formic acid. Samples were analyzed by tandem mass spectrometry (MS/MS). Briefly, peptides were resolved in a gradient of 4–95% (v/v) MeCN using reverse phase high performance liquid chromatography, using the UltiMate 3000 system (Dionex, Camberley, UK). Samples were acquired on a 4000 Q TRAP® liquid chromatography/MS/MS system (Applied Biosystems, Warrington, UK). Data were analyzed using Analyst® software (Applied Biosystems).

Immunoprecipitation—Peak fractions from the HiTrap SP-Sepharose HP cation exchanger column (25 μl) were incubated with primary antibody (0.25–2 μl VC1 antibody to VRK1 or antibody to CK1α) overnight at 4 °C in immunoprecipitation buffer (0.1% (w/v) SDS, 1% (v/v) Nonidet P-40, 50 mM Tris-HCl (pH 7.4), 150 mM NaCl, 1 mM EDTA) in a final volume of 50 μl. Protein G-Sepharose Fast Flow beads (50 μl) were then added, and the reactions were incubated at 4 °C for a further 2 h. The flow-through was collected and assayed for *in vitro* kinase activity toward FLp53 tetramers, and the beads were washed six times in 100 μl of immunoprecipitation buffer. Bound protein was eluted after a 45-min incubation in 100 μl of elution buffer (SDS sample buffer containing 0.2 M DTT) at room temperature. Negative control reactions, where the antibody was omitted, were included.

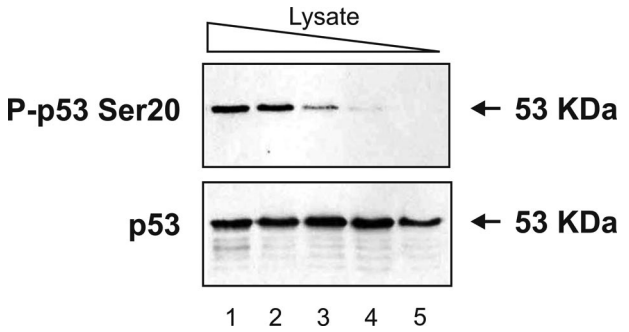

FIGURE 1. **HHV-6B-infected MOLT-3 lysates display cell-free p53 Ser^{20} kinase activity.** MOLT-3 cells were infected with HHV-6B for 48 h prior to lysis. Decreasing amounts of the whole-cell lysates (10-fold serial dilutions in *lanes 1–5*) acted as the kinase source in an *in vitro* kinase assay using recombinant FLp53 tetramers as the substrate. Kinase assay samples were subjected to Western blotting using P-p53 Ser^{20} (*top*) and DO-12 (*bottom*) antibodies to detect FLp53 phosphorylated at Ser^{20} and total FLp53, respectively.

RESULTS

HHV-6B-infected MOLT-3 Cells Contain a Kinase That Displays Ser^{20} Site Activity toward p53 in Vitro—HHV-6B infection has previously been shown to induce Ser^{20} site phosphorylation of p53, although the kinase that mediates this stress-activated phosphorylation has not been identified (14). We set out to determine whether HHV-6B-infected MOLT-3 cell lysates were capable of mediating the phosphorylation of p53 at Ser^{20} in an *in vitro* assay. HHV-6B-infected MOLT-3 whole-cell lysates acted as the kinase source in an *in vitro* kinase assay using recombinant FLp53 tetramers as the substrate. Western blotting of the kinase assay products revealed that p53 was phosphorylated at Ser^{20} (Fig. 1, *lanes 1–4*) and that the amount of P-p53 Ser^{20} was proportional to the amount of kinase source used in the kinase assay. HHV-6B-infected MOLT-3 cell lysates therefore contain at least one kinase that is capable of mediating the phosphorylation of p53 at Ser^{20} *in vitro*.

In order to identify the p53 Ser^{20} kinase, we subjected crude lysates to chromatographic fractionation to determine whether the kinase activity correlates with the known Ser^{20} site kinases, including CHK1/2 and DAPK-1. HHV-6B-infected and mock-infected MOLT-3 whole-cell lysates were applied onto a Q-Sepharose Fast Flow anion exchanger column, proteins were eluted in a linear gradient of 0–1 M KCl, and fractions were collected and assayed for kinase activity toward the Ser^{20} and Ser^{15} sites of FLp53 (Fig. 2). The induction of Ser^{20} site phosphorylation correlated with an increase in the specific activity of the Ser^{20} site kinase. The kinase eluted from fractions 14–18 in mock-infected cells (Fig. 2*A*, *upper panels*, *lanes 9–11*), whereas in HHV-6B-infected cells, the kinase eluted from fractions 10–20 (Fig. 2*A*, *lower panels*, *lanes 7–12*) and a broader elution peak from fractions 26–48 (*lanes 15–26*). By contrast, the induction of Ser^{15} site phosphorylation after HHV-6B infection did not exhibit the same qualitative increase in cell-free kinase activity (Fig. 2*B*). When these fractions containing the peak Ser^{20} site kinase activity were immunoblotted for the kinases known to phosphorylate p53 Ser^{20}, none of the calcium calmodulin kinase superfamily members co-eluted precisely with the Ser^{20} site kinase activity (data not shown). Thus, we

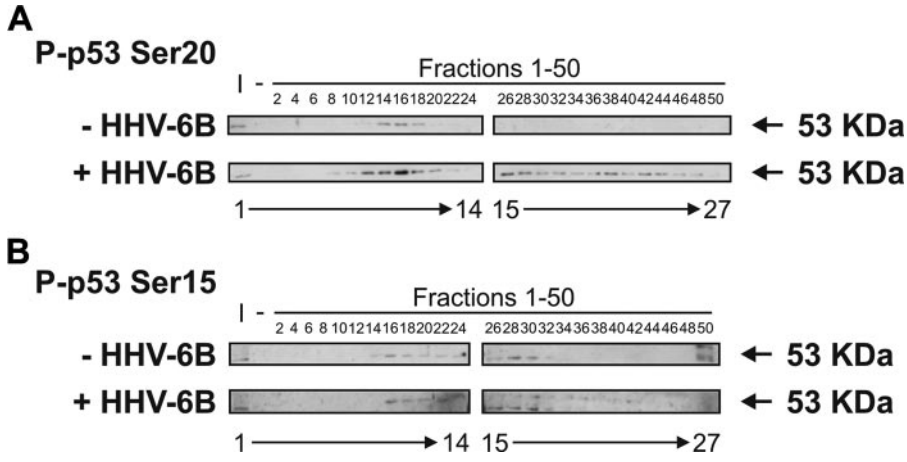

FIGURE 2. **p53 Ser^{20} kinase activity is elevated in HHV-6B-infected MOLT-3 cell lysates.** Mock-infected (*top*) and HHV-6B-infected (*bottom*) MOLT-3 whole-cell lysates were subjected to chromatographic fractionation using a Q-Sepharose Fast Flow anion exchanger with a linear gradient of 0–1 M KCl. Even-numbered fractions (*lanes 3–27*) were assayed for *in vitro* kinase activity toward recombinant FLp53 tetramers, and Western blotting using P-p53 Ser^{20} and P-p53 Ser^{15} antibodies revealed phosphorylation at the Ser^{20} (*A*) and Ser^{15} (*B*) sites of FLp53. *Input* (*I*; *lane 1*) and negative (−; *lane 2*) controls were included and consisted of unfractionated whole-cell lysates and distilled H_2O as the kinase source, respectively.

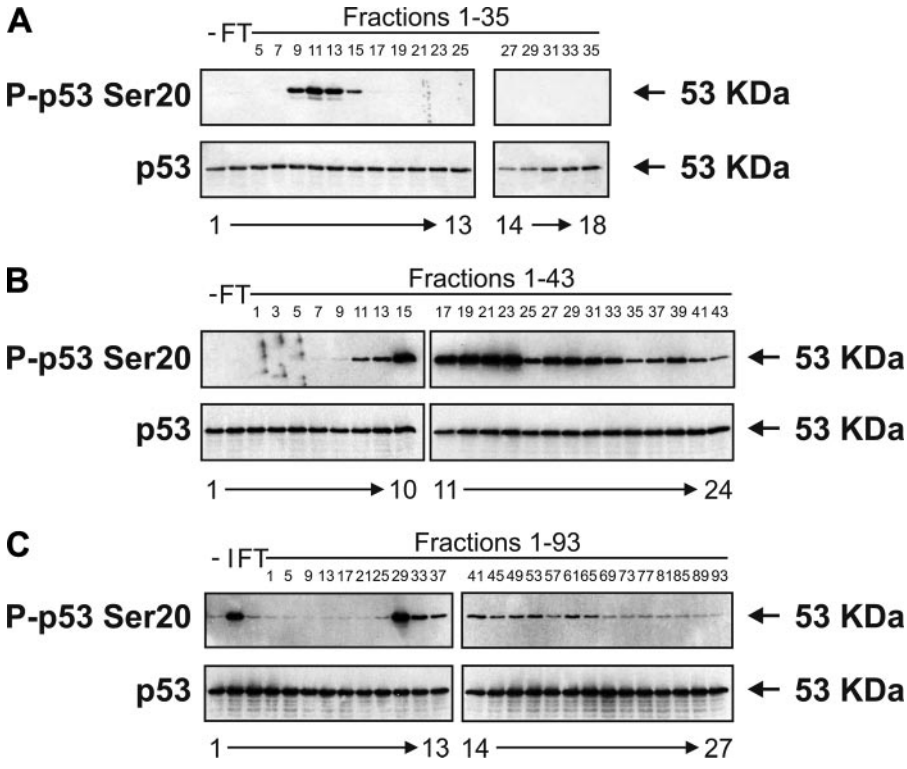

FIGURE 3. **Purification of the virus-induced p53 Ser20 kinase.** *A*, HHV-6B-infected MOLT-3 whole-cell lysates were subjected to chromatographic fractionation using a Q-Sepharose Fast Flow anion exchanger with a linear gradient of 0–1 M KCl. The column flow-through (*FT*; *lane 2*) and odd-numbered fractions (*lanes 3–18*) were assayed for *in vitro* kinase activity toward the Ser^{20} site of FLp53 tetramers, which was detected by Western blotting using P-p53 Ser^{20} (*top*) and DO-12 (*bottom*) antibodies. A negative control (−; *lane 1*), consisting of distilled H_2O as the kinase source, was included. *B*, fractions 9–14 from *A* were pooled and subjected to further chromatographic fractionation using a Reactive Brown 10-agarose cation exchanger with a linear gradient of 0.01–2 M KCl. The column flow-through (*lane 2*) and odd-numbered fractions (*lanes 3–24*) were assayed for *in vitro* kinase activity toward the Ser^{20} site of FLp53 tetramers, which was detected by Western blotting using P-p53 Ser^{20} (*top*) and DO-12 (*bottom*) antibodies. A negative control (−; *lane 1*), consisting of distilled H_2O as the kinase source, was included. *C*, fractions 17–23 from *B* were pooled and subjected to a final chromatographic fractionation using a HiTrap SP-Sepharose HP cation exchanger with a linear gradient of 0.01–2 M KCl. The column flow-through (*lane 3*) and every fourth fraction (*lanes 4–27*) were assayed for *in vitro* kinase activity toward the Ser^{20} site of FLp53 tetramers, which was detected by Western blotting using P-p53 Ser^{20} (*top*) and DO-12 (*bottom*) antibodies. Negative (−; *lane 1*) and input (*I*; *lane 2*) controls were included and consisted of distilled H_2O and pooled fractions 17–23 from *B* as the kinase source, respectively.

set up further chromatographic fractionations in order to enrich the HHV-6B-induced Ser^{20} site kinase activity sufficiently to identify candidate leads by identifying protein bands from SDS-PAGE gels using mass spectrometry (MS).

Purification of the p53 Ser^{20} Kinase—Large scaled up samples of HHV-6B-infected MOLT-3 whole-cell lysates were applied onto a Q-Sepharose Fast Flow anion exchanger column, proteins were eluted in a linear gradient of 0–1 M KCl, and fractions were collected and assayed for kinase activity toward the Ser^{20} site of FLp53 (Fig. 3*A*). Fractions 9–14 containing the most activity (Fig. 3*A*, *lanes 5–8*) were pooled and applied onto a Reactive Brown 10-agarose cation exchange column. Proteins were eluted in a linear gradient of 10 mM to 2 M KCl, and fractions were collected and assayed for kinase activity toward FLp53 Ser^{20}, as described previously (Fig. 3*B*). Fractions 17–23 containing the first peak of activity (Fig. 3*B*, *lanes 11–14*) were pooled and applied onto a HiTrap SP-Sepharose HP cation exchanger column. Proteins were eluted in a linear gradient of 10 mM to 2 M KCl, and fractions were again collected and assayed for kinase activity toward FLp53 Ser^{20} (Fig. 3*C*). Fraction 29 displayed the most activity toward FLp53 Ser^{20} (Fig. 3*C*, *lane 11*).

The p53 Ser^{20} Kinase Is CK1α—None of the calcium calmodulin kinase superfamily members co-eluted with the fractions from the HiTrap SP-Sepharose HP cation exchanger column that displayed the peak of p53 Ser^{20} kinase activity (Fig. 4, *lane 10*). As such, we resolved protein from the peak fractions by SDS-PAGE, and after staining with colloidal blue (Fig. 5*A*, *left*), we excised and processed the proteins that were enriched in the peak fraction (Fig. 5*A*, *right*, *lane 5 versus lane 4* or *6*) for analysis by MS in order to acquire candidate kinase leads. MS identified VRK1 (47 kDa) and CK1α (38 kDa) as candidate

kinases that eluted in fraction 31 (Fig. 5, *B* and *C*), a fraction that displayed strong kinase activity toward the Ser[20] site of FLp53.

Western blotting confirmed that the elution profiles of CK1 or CK1α (Fig. 6, *A* and *B*) and VRK1 (Fig. 6*C*) matched the p53 Ser[20] kinase activity profile. CK1 and CK1α eluted mostly in fraction 29 (Fig. 6, *A* and B, *lanes 10* and *9*, respectively), and VRK1 eluted in fractions 29–33 (Fig. 6*C*, *lanes 10* and *11*), suggesting that either kinase could be responsible for the observed phosphorylation of FLp53 at Ser[20] in the peak fraction 29 (Fig. 3*C*). Immunoprecipitation studies revealed that the kinase activity toward FLp53 at Ser[20] was attenuated after immunodepletion of CK1α (Fig. 7*A*, *lanes 4–7 versus lane 3*) and not after depletion of VRK1 (Fig. 7*A*, *lanes 9–12 versus lane 8*), implying that CK1α is the dominant p53 Ser[20] kinase. This agrees with previous data showing that recombinant VRK1 does not exhibit Ser[20] site kinase activity (10). However, this does rule out VRK1 as a co-purifying subunit of CK1. As controls, we affirmed that increasing the antibody titration did result in reduced CK1α (Fig. 7*B*, *lanes 2–5 versus lane 1*) and VRK1 (Fig. 7*C*, *lanes 2–5 versus lane 1*) in the immunodepleted samples as well as elevated CK1α (Fig. 7*B*, *lanes 7–10 versus lane 6*) and VRK1 (Fig. 7*C*, *lanes 7–10 versus lane 6*) in the immune pellet.

Together, these results demonstrate that CK1α is the most likely cellular virus-induced Ser[20] site kinase. However, we still set up assays to compare recombinant CK1δ kinase domain purified from *Escherichia coli* with the native enzyme purified from MOLT-3 cells in order to determine whether the native enzyme has the same properties as the recombinant CK1. Recombinant CK1δ was able to mimic the native enzyme and catalyze Ser[20] site phosphorylation of FLp53 tetramers *in vitro* (Fig. 8*A*, *lane 5 versus lane 3*). This finding is consistent with the original data on CK1δ, which showed that mutation of p53 at Ser[20] is sufficient to block completely p53 phosphorylation (11). We could not detect p53 Thr[18] phosphorylation induced by native or recombinant CK1 using a well validated Thr[18]-phosphospecific monoclonal antibody (Fig. 8*B*, *lanes 3* and *5*), which might be expected, since recombinant CK1δ-mediated phosphorylation at Thr[18] requires a prior phosphorylation of p53 at Ser[15] by phosphoinositide 3-kinases (11).

The Phosphorylation of p53 at Ser[20] by Native CK1α Is Dependent on Interactions with the BOX-IV and BOX-V Domains of p53—All enzymes reported to modify the Thr[18] or Ser[20] sites within the *BOX-I* domain of p53 to date also interact with the multiprotein docking site in the *BOX-V* domain of p53 (Fig. 9). The three-dimensional proximity of the *BOX-V* motif to the *BOX-I* motif in tetrameric p53 is not known. However, synthetic peptide fragments from the *BOX-V* domain of p53 can alter in *trans* the *BOX-I* Ser[20] site kinase activity of the

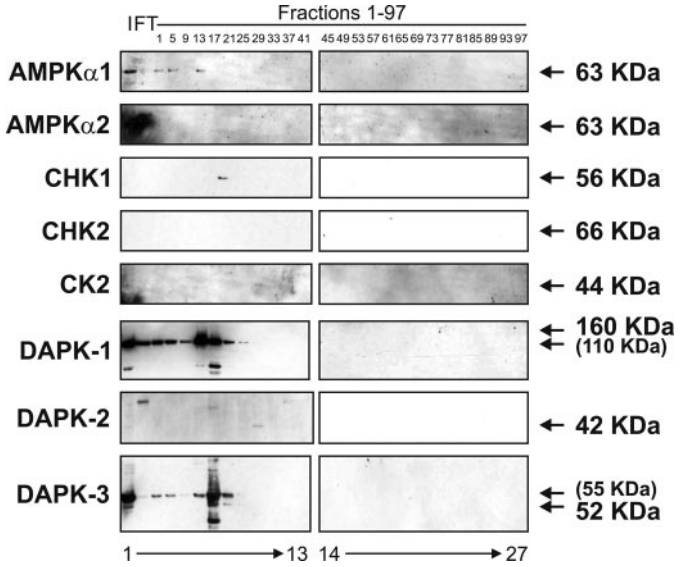

FIGURE 4. **Calcium calmodulin kinases do not co-elute with virus-induced p53 Ser[20] kinase activity.** The flow-through (*FT*; *lane 2*) and every fourth fraction (*lanes 3–27*) from the HiTrap SP-Sepharose HP cation exchanger column were subjected to Western blotting with antibodies against known calcium calmodulin kinase superfamily members (AMPKα1, AMPKα2, CHK1, CHK2, CK2, DAPK-1, DAPK-2, and DAPK-3). An input control (*I*; *lane 1*), consisting of pooled fractions 17–23 from the Reactive Brown 10-agarose cation exchanger column, was included.

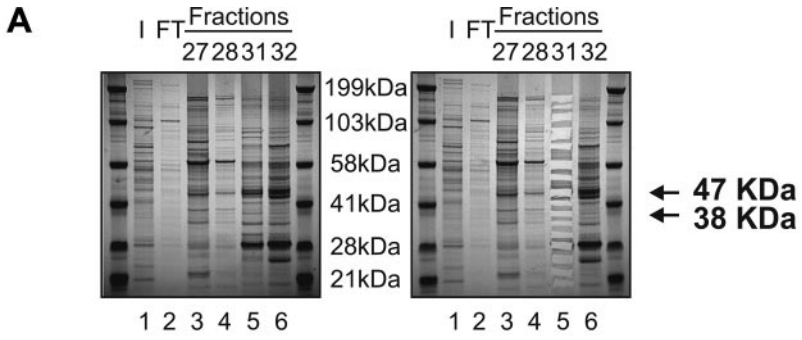

B

VRK1 Peptide Hits	Observed Molecular Weight	Expected Molecular Weight	Calculated Molecular Weight	Delta	Probability Based Mowse Score
ASNLLLNYK	518.2310	1034.4475	1034.5760	-0.1285	58
VEPSDNGPLFTELK	773.2886	1544.5626	1544.7722	-0.2095	20
CHDGTIEFTSIDAHNGVAPSR	571.9659	2283.8344	2283.0338	0.8006	26

C

CK1α Peptide Hits	Observed Molecular Weight	Expected Molecular Weight	Calculated Molecular Weight	Delta	Probability Based Mowse Score
ILQGGVGIPHIR	630.4056	1258.7967	1258.7509	0.0457	23
TVLMLADQMIAR	697.4793	1392.9441	1392.7105	0.2336	36

FIGURE 5. **Mass spectrometry identifies VRK1 and CK1α as candidate p53 Ser[20] kinases.** *A*, the flow-through (*FT*; *lane 2*) and concentrated fractions 27, 28, 31, and 32 (*lanes 3–6*) from the HiTrap SP-Sepharose HP cation exchanger column were resolved by SDS-PAGE and stained with colloidal blue (*left*). An input control (*I*; *lane 1*), consisting of pooled fractions 17–23 from the Reactive Brown 10-agarose cation exchanger column, was included. Proteins enriched in fraction 31 (*lane 5*) were excised from the gel (*right*) and processed for analysis by MS/MS. *B* and *C*, MS identified VRK1 (*B*) and CK1α (*C*) as candidate kinases.

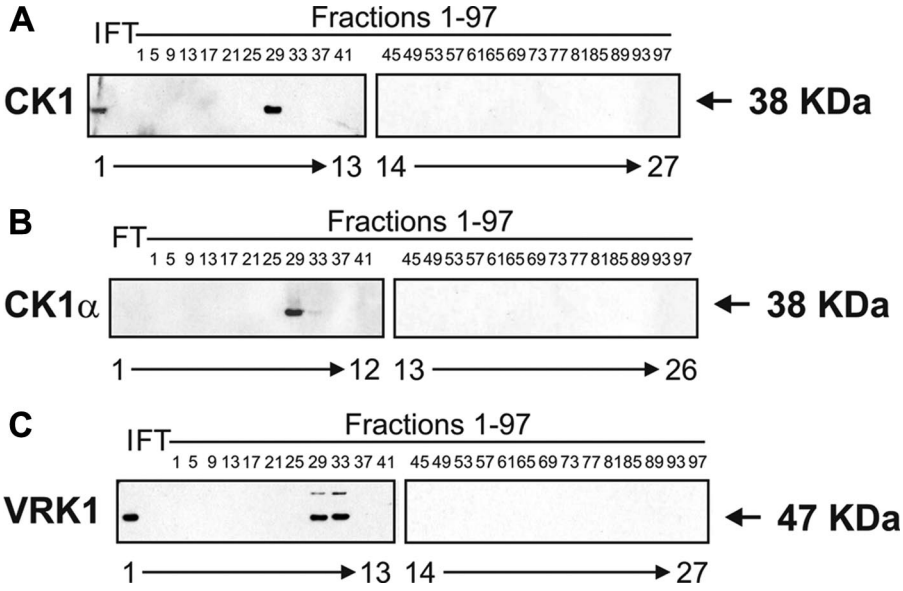

FIGURE 6. **CK1, CK1α, and VRK1 co-elute with p53 Ser^{20} kinase activity.** The flow-through (*FT*; *lanes 1* and *2*) and every fourth fraction (*lanes 2–26* or *3–27*) from the HiTrap SP-Sepharose HP cation exchanger column were subjected to Western blotting with antibodies against CK1 (*A*), CK1α (*B*), or VRK1 (*C*). An input control (*I*; *lane 1*), consisting of pooled fractions 17–23 from the Reactive Brown 10-agarose cation exchanger column, was included in *A* and *C*.

respective enzymes (18, 19). Kinase assays were performed using peptides designed to the *BOX-IV* and *BOX-V* domains of the coding sequence of human p53 (Fig. 9 and Table 1) in order to monitor peptide stimulation or inhibition of kinase function toward FLp53 tetramers (Fig. 10). Several peptides (peptides 2–4, 12 and 13, and 16 and 17) had an inhibitory effect on the kinase activity of CK1α toward the Ser^{20} site of FLp53 tetramers (Fig. 10*A*, lanes 5–7, 15 and 16, and 19 and 20). This implies that residues 251–253, 261–262, and 265–266 of p53 encompass docking sites in the *BOX-IV* and *BOX-V* domains that are crucial for the Ser^{20} site activity of CK1α. The location of these key docking sites within the localized three-dimensional structure of p53 is shown in Fig. 10*C*.

Distinct Residues in the BOX-IV and BOX-V Domains of p53 Are Important for the Interaction of p53 with Different Proteins—We evaluated whether DAPK-1 core domain has a similar or overlapping sensitivity to the p53 *BOX-IV* and *BOX-V* peptides as native CK1α. Several peptides (peptides 4 and 5, 13–16, and 18) had an inhibitory effect on the kinase activity of DAPK-1 core toward the Ser^{20} site of FLp53 tetramers (Fig. 10*B*, *lanes 7* and *8*, 16–19, and 21). This implies that residues 253–254, 262–265, and 267 in the *BOX-IV* and *BOX-V* domains of p53 are important for the Ser^{20} site activity of DAPK-1 core. The location of these key docking sites within the three-dimensional structure of p53 is shown in Fig. 10*D*. These data indicate that at least two distinct kinases have an overlapping, but nonidentical, interaction with the *BOX-IV* and *BOX-V* domains of p53.

CK1 Inhibitors Attenuate p53 Induction by HHV-6B Infection—In order to obtain independent genetic evidence that CK1 is the major Ser^{20} site kinase for p53 in HHV-6B-infected cells, we needed to inhibit the enzyme to determine whether p53 induction would be reduced. The MOLT-3 cells are well known to be difficult to transfect using small interfering RNA, so we could not deplete endogenous CK1 using this approach. However, there are three chemical inhibitors of CK1 that can be used, one of which (D4476) shows a more pronounced specificity for CK1 (31). Upon increasing addition of D4476 to HHV-6B-infected MOLT-3 cells, there was a dose-dependent reduction in Ser^{20} site phosphorylation (Fig. 11*A*, *top*, *lanes 4–14 versus lane 2*). This reduction was especially pronounced from a concentration of 20 μM D4476 and higher (Fig. 11*A*, *top*, *lanes 6–14 versus lane 2*). This inhibition of p53 Ser^{20} site phosphorylation did not result in loss of CK1 enzyme (Fig. 11*A*, *third panel*, *lanes 4–14 versus lane 2*); however, there was an increase in a higher molecular weight adduct at the 20 μM concentration of D4476 irrespective of HHV-6B infection status (Fig. 11*A*, *third panel*, *lanes 5* and *6 versus lanes 1* and *2*).

Although previous studies were unable to show a reduction in HHV-6B-induced phosphorylation of p53 at Ser^{15}, Ser^{20}, or Ser^{392} using chemical inhibitors designed to CK2, double-stranded RNA-activated protein kinase, or p38 mitogen-activated protein kinase (15), we evaluated whether CK1 inhibition of Ser^{20} site phosphorylation could be uncoupled from HHV-6B-induced phosphorylation at other sites. At the concentrations of D4766 where we began to observe reductions in Ser^{20} site phosphorylation (10 and 20 μM), there was no reduction detected in HHV-6B induction of Ser^{15} or Ser^{392} phosphorylation of p53 (Fig. 11, *B* and *C*, *top*, *lanes 4* and *6 versus lane 2*). However, from a concentration of 40 μM D4476 and higher, there was a complete inhibition of HHV-6B-induced Ser^{15} site phosphorylation (Fig. 11*B*, *top*, *lanes 8–14*) but not Ser^{392} site phosphorylation (Fig. 11*C*, *top*, *lane 8*). Only at concentrations of 60 μM D4476 or higher did we see inhibition of Ser^{392} site phosphorylation of p53 (Fig. 11*C*, *top*, *lanes 10–14 versus lane 2*). Together, these data suggest that CK1 may not only be the Ser^{20} site kinase after virus infection but that there might be a degree of cross-talk between CK1 and the enzymes that mediate p53 phosphorylation at Ser^{15} and Ser^{392}.

CK1 Inhibitors Do Not Attenuate p53 Induction by X-ray Treatment—We next set out to determine whether CK1 is a global Ser^{20} site kinase for p53 in response to a wide range of stresses or whether CK1 acts specifically in response to viral infection. MOLT-3 cells were therefore treated with and without a 6-gray x-ray in the presence of increasing amounts of the CK1 inhibitor D4476. Although x-rays induced the phosphorylation of p53 at Ser^{20} along with an increase in p53 levels (Fig. 12, *even-numbered lanes versus odd-numbered lanes*), increasing the addition of D4476 did not attenuate either the Ser^{20} site phosphorylation or the induction of p53 (Fig. 12, *lanes 6–12*

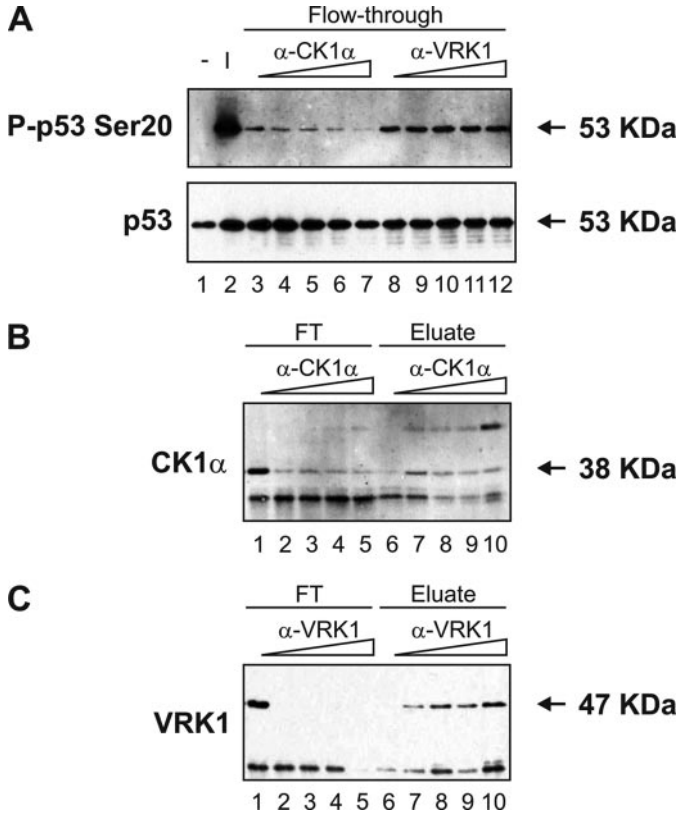

FIGURE 7. **Immunodepletion of CK1α, but not VRK1, abolishes p53 Ser^{20} kinase activity.** CK1α or VRK1 were immunoprecipitated from a peak fraction from the HiTrap SP-Sepharose HP cation exchanger column using increasing amounts (0.25–2 μl) of antibody to CK1α or VRK1 bound to Protein G-Sepharose Fast Flow beads. *A*, immunodepleted fractions, or flow-through (*FT*; *lanes 3–12*), were assayed for *in vitro* kinase activity toward the Ser^{20} site of FLp53 tetramers, which was detected by Western blotting using P-p53 Ser^{20} (*top*) and DO-12 (*bottom*) antibodies. Negative (−; *lane 1*) and input (*I*; *lane 2*) controls were included and consisted of distilled H_2O and the peak fraction as the kinase source, respectively. Fractions depleted of CK1α and VRK1 are shown in *lanes 4–7* and *lanes 9–12*, respectively, and negative control reactions, where the antibody was omitted, are shown in *lanes 3* and *8*. *B* and *C*, immunodepleted fractions, or flow-through (*lanes 1–5*), and the corresponding immune pellet, or eluate (*lanes 6–10*), were subjected to Western blotting with antibodies to CK1α (*B*) or VRK1 (*C*). Fractions depleted of CK1α and VRK1 are shown in *B* and *C*, respectively, and negative control reactions, where the antibody was omitted from the immunoprecipitation reactions, are shown in *lanes 1* and *6*.

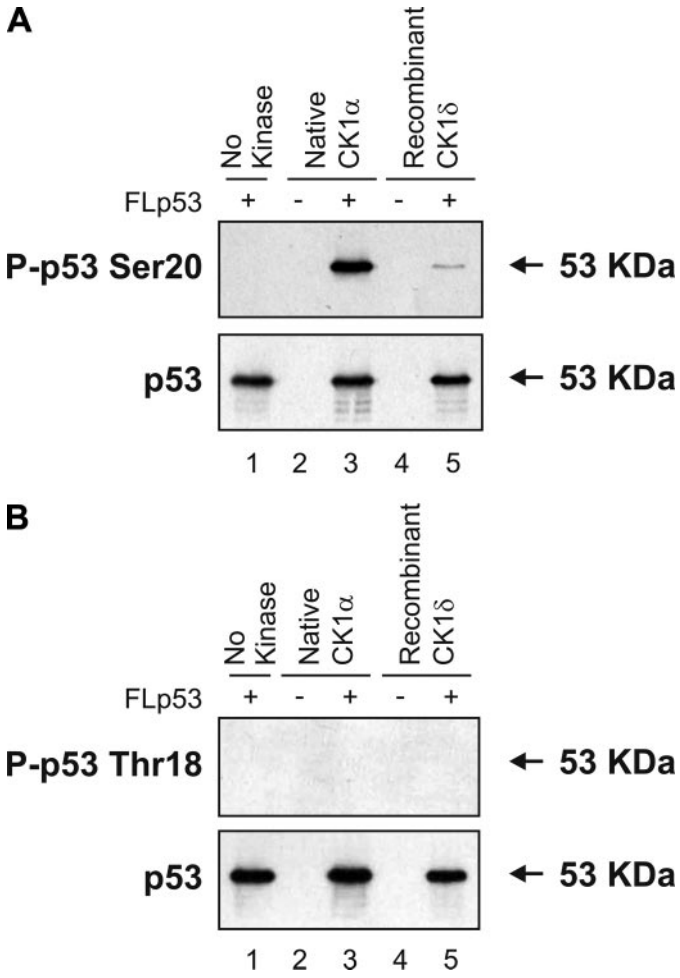

FIGURE 8. **Native and recombinant CK1 phosphorylate p53 at Ser^{20}.** Native CK1α purified from HHV-6B-infected MOLT-3 cells (*lanes 2* and *3*) or recombinant GST-CK1δ kinase domain purified from *E. coli* (*lanes 4* and *5*) was assayed for *in vitro* kinase activity toward the Ser^{20} (*A*) and Thr^{18} (*B*) sites of FLp53 tetramers, which was detected by Western blotting using P-p53 Ser^{20} (*A*, *top*), P-p53 Thr^{18} (*B*, *top*), and DO-12 (*A* and *B*, *bottom*) antibodies. Negative control reactions, lacking either the kinase source (*lane 1*) or the kinase substrate (*lanes 2* and *4*) were included.

versus lanes 2 and *4*). The data therefore suggest that CK1 is a virus-specific Ser^{20} site kinase for p53 and that other kinases are responsible for mediating the phosphorylation of p53 at Ser^{20} after distinct stresses, such as x-rays.

DISCUSSION

The p53 tetramer is subject to a complex set of diverse post-translational modifications that are induced in a coordinated manner by stress-activated pathways. These covalent adducts include phosphorylation, ubiquitination, acetylation, additional ubiquitin-like modifications, and methylation. These modifications occur within different domains of the p53 protein and result in distinct effects both on the tetrameric conformation and the protein interaction network of p53, and they ultimately affect the specific activity of p53. These post-translational modifications are catalyzed by a range of enzymes, including p300, UBCH5/Mdm2, cyclin-dependent kinases, CK2, and CHK2. A feature of these enzymatic modifications is that they occur through enzyme docking to multiple linear peptide interaction sites within the p53 tetramer (2). Presumably, p53 has therefore evolved these unstructured and flexible motifs common to regulatory enzymes in order to coordinate multiple stress-activated signaling events.

Since phosphorylation of the Ser^{20} site of p53 plays a dominant role in stabilizing p300 and mediating DNA-dependent acetylation of p53, as well as B-cell lymphoma suppression, it is of interest to define the environmental stresses and the kinases that mediate this phosphorylation. Studies originally highlighted that CHK1 and CHK2 were the major Ser^{20} kinases for p53, although this has been questioned (20, 21). Subsequent work has shown that members of the calcium calmodulin kinase superfamily, including CHK1, CHK2, AMPK (AMP-activated protein kinase), DAPK-1, DAPK-3, and DRAK-1 (DAPK-related 1) can phosphorylate the Thr^{18} and/or Ser^{20} residues of p53 in a cell-free assay (18). These kinases, including CHK1/2, modify p53 in a dual site docking-dependent manner. This shows that phosphorylation events within the *BOX-I* domain of p53 are dependent on kinase docking interactions

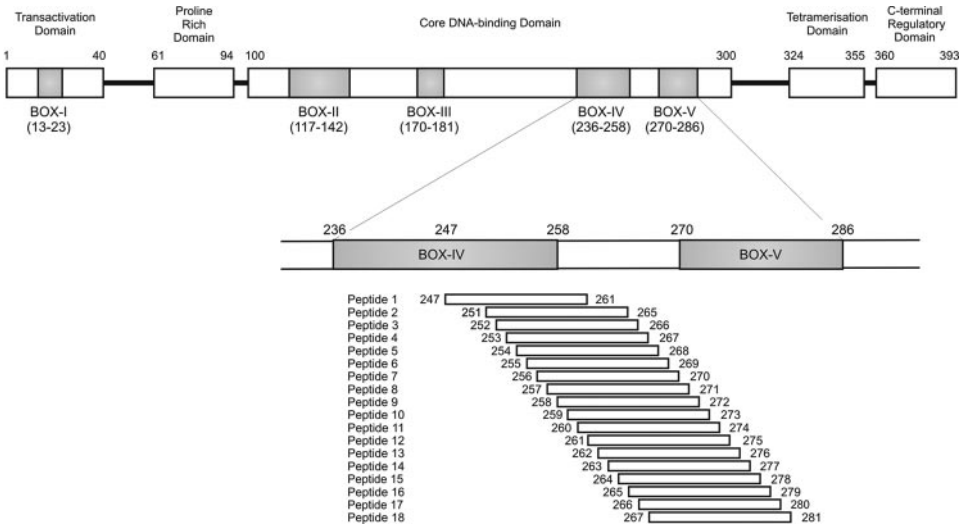

FIGURE 9. **Location of the synthetic peptides within the coding sequence of p53.** The domain structure of p53 (393 amino acids) is represented, including the conserved domains, labeled with the indicated amino acids flanking *BOX-I* through *BOX-V*. Overlapping synthetic 15-mer peptides were designed to the *BOX-IV* and *BOX-V* domains of the coding sequence of human p53. See Table 1 for peptide sequences.

TABLE 1

p53 peptide amino acid sequences

Shown are overlapping synthetic 15-mer peptides from the coding sequence of human p53. All peptides were biotinylated at the N terminus with SGSG spacers and had a C terminal amide group.

Peptide	Sequence
Peptide 1	NRRPILTIITLEDSS
Peptide 2	ILTIITLEDSSGNLL
Peptide 3	LTIITLEDSSGNLLG
Peptide 4	TIITLEDSSGNLLGR
Peptide 5	IITLEDSSGNLLGRN
Peptide 6	ITLEDSSGNLLGRNS
Peptide 7	TLEDSSGNLLGRNSF
Peptide 8	LEDSSGNLLGRNSFE
Peptide 9	EDSSGNLLGRNSFEV
Peptide 10	DSSGNLLGRNSFEVR
Peptide 11	SSGNLLGRNSFEVRV
Peptide 12	SGNLLGRNSFEVRVC
Peptide 13	GNLLGRNSFEVRVCA
Peptide 14	NLLGRNSFEVRVCAC
Peptide 15	LLGRNSFEVRVCACP
Peptide 16	LGRNSFEVRVCACPG
Peptide 17	GRNSFEVRVCACPGR
Peptide 18	RNSFEVRVCACPGRD

within the conformationally flexible *BOX-V* domain of p53 (model depicted in Fig. 13*A*). Similarly, recent work has also shown that the ubiquitination of p53 by Mdm2 is regulated by a related dual site mechanism. Stimulation of the ubiquitin ligase function of Mdm2 requires the interaction of Mdm2 both with the *BOX-I* domain of p53 and with a ubiquitination signal found within the *BOX-V* domain of p53 (22). It is therefore becoming increasingly apparent that the *BOX-V* domain of p53 is a key multiprotein docking region, equivalent to the *BOX-I* domain, with both activating kinases and negative regulators potentially competing for binding to overlapping motifs (Fig. 13*A*).

Although DNA damage induced by radiation has been the most well characterized stress that activates p53, perhaps more biologically intrinsic stresses have also been reported that have not been as well dissected. These include hypoxia, interferon-signaling, and DNA or RNA virus infection. A range of DNA or RNA viruses can induce p53-dependent apoptosis in some cell types (23, 24). Further, type I interferons can activate p53-dependent processes in animal models (12). Whether these interferon signaling effects occur in dendritic cells and/or macrophages and how this alters immune system integrity in either normal or cancer cells remains to be determined. The link between p53 and interferon or virus responses is particularly intriguing, since a role for p53 in immunity might have been the physiological selection pressure under which the p53 pathway appeared during evolution in chordates. This would have occurred evolutionarily to maintain host survival during viral or pathogen infection. Indeed, some tumor viruses have evolved proteins that bind to and inactivate or degrade p53, thus permitting virus propagation. Understanding the kinase signaling pathways that cells use to activate p53 after virus infection should provide fundamental insights into the physiology of the p53 response to immune system stresses. Although there is a range of RNA and DNA viruses that have been reported to activate p53-dependent processes, we have used HHV-6B as a model. This virus is thought to be the most ancient, founding member of the HHV family of viruses and has the unusual property of inducing growth arrest rather than apoptosis in infected T-cells (14, 25).

HHV-6B has previously been reported to induce phosphorylation of p53 at Ser^{15}, Ser^{20}, Ser^{33}, and Ser^{392} (14, 15). Phosphorylation at Thr^{18} after viral infection cannot be detected in this system (data not shown). Of these sites, the Ser^{20} and Ser^{392} phosphoacceptor site mutations have been made in animal transgenic models and result in stress-induced or cell-specific tumor-prone phenotypes (7–9). The Ser^{20} phosphoacceptor site has appeared rather late in evolution, since it is found only in mammals. The phosphorylation of p53 at Ser^{20} has the most striking effect in stabilizing the binding of p300 (4), which in turn stimulates the DNA-dependent acetylation of p53 (3, 26). Interestingly, although the Ser^{20} site is confined to mammals, certain fish species have evolved a negatively charged amino acid at this position, suggesting that other vertebrates also exploit this site to anchor p300. Defining which kinase pathway(s) targets the Ser^{20} site after viral infection will help us to identify potential evolutionarily core signaling pathways that have maintained mammalian host survival under the natural selection imposed by virus infection.

In this report, we identify CK1α as the dominant enzyme that catalyzes Ser^{20} site phosphorylation of p53 after viral infection. This conclusion is based on (i) the purification of the virus-induced Ser^{20} site kinase away from the known Ser^{20} site kinases, including CHK1/2 and DAPK-1, (ii) the immunodepletion of p53 Ser^{20} kinase activity from infected cell lysates, and (iii) the ability of a relatively specific CK1 inhibitor to attenuate virus-induced Ser^{20} site phosphorylation in cells. Like all

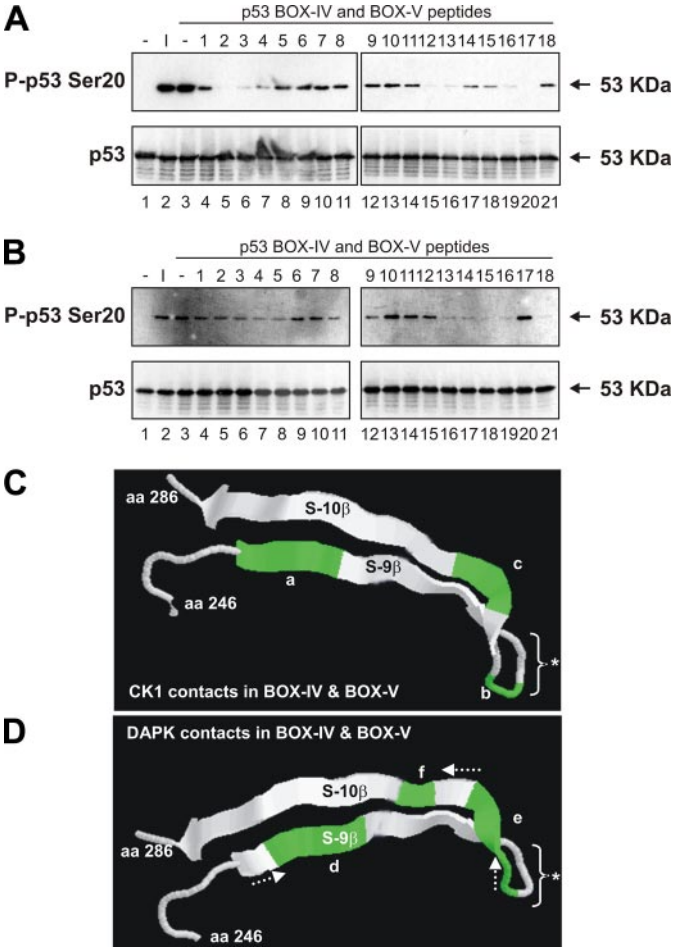

FIGURE 10. **The *BOX-IV* and *BOX-V* domains of p53 act as multiprotein docking sites necessary for the p53 Ser^{20} kinase activity of CK1α and DAPK-1.** *A* and *B*, native CK1α purified from HHV-6B-infected MOLT-3 cells (*A*) or DAPK-1 core domain (*B*) were assayed for *in vitro* kinase activity toward the Ser^{20} site of FLp53 tetramers in the presence of p53 *BOX-IV* and *BOX-V* peptides (*lanes 4–21*) or a DMSO solvent control (*lane 3*). Western blotting using P-p53 Ser^{20} (*top*) and DO-12 (*bottom*) antibodies revealed FLp53 phosphorylated at Ser^{20} and total FLp53, respectively. Negative control reactions (−; *lane 1*) lacking the kinase source and positive or input controls (*I*; *lane 2*) with the kinase source were included. *C* and *D*, location of key CK1α (*C*) or DAPK-1 (*D*) docking sites within the *BOX-IV* and *BOX-V* domains of the three-dimensional structure of p53 that are necessary for the p53 Ser^{20} kinase activity of either CK1α (*C*) or DAPK-1 (*D*). *Highlighted* docking regions encompass residues 251–253 (*a*), 261 and 262 (*b*), 265 and 266 (*c*), 253 and 254 (*d*), 262–265 (*e*), and 267 (*f*). The *arrows* indicate the shift in docking site preferences of DAPK-1 *versus* CK1α. *, the conformationally flexible monoclonal antibody epitope, which can be exposed or cryptic, depending upon p53 conformation. *aa*, amino acids.

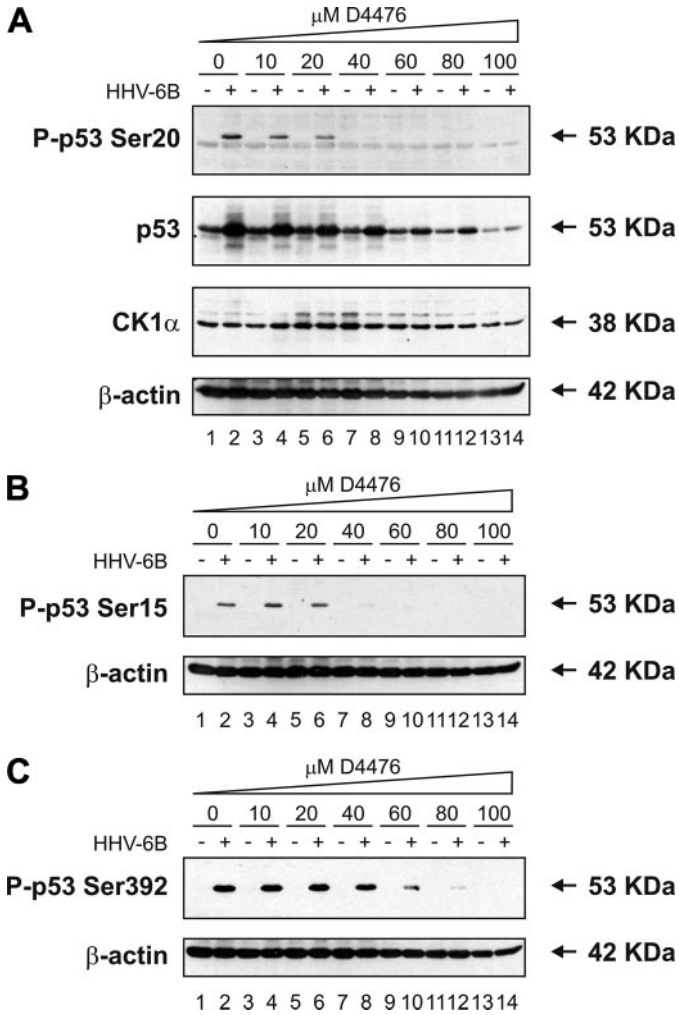

FIGURE 11. **A CK1 inhibitor attenuates Ser^{20} site phosphorylation of p53 and p53 induction mediated by HHV-6B infection.** *A–C*, MOLT-3 cells were infected with (*even-numbered lanes*) or without (*odd-numbered lanes*) HHV-6B for 48 h in the presence of increasing concentrations (10–100 μM) of the CK1 inhibitor D4476 (*lanes 3–14*) or a DMSO solvent control (*lanes 1* and *2*). Cell lysates were examined by Western blotting with antibodies against the indicated proteins.

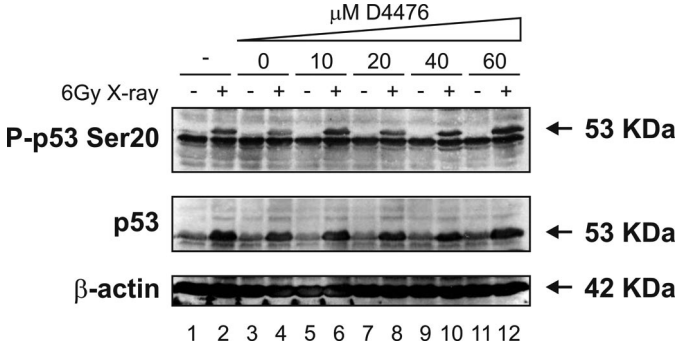

FIGURE 12. **A CK1 inhibitor does not attenuate Ser^{20} site phosphorylation of p53 and p53 induction mediated by treatment with x-rays.** MOLT-3 cells were treated with (*even-numbered lanes*) or without (*odd-numbered lanes*) 6-gray x-ray and cultured for 4 h after an initial 44-h pretreatment with increasing concentrations (10–60 μM) of the CK1 inhibitor D4476 (*lanes 5–12*), a DMSO solvent control (*lanes 3* and *4*), or a culture medium control (*lanes 1* and *2*). Cell lysates were examined by Western blotting with antibodies against the indicated proteins.

enzymes reported to modify the Thr^{18} or Ser^{20} sites of p53 to date, CK1α also interacts with the multiprotein docking site in the *BOX-V* domain of p53 (model illustrated in Fig. 13*A*). Further, despite the fact that CK1 can catalyze p53 phosphorylation at Thr^{18} (27), with a prior DNA damage-inducible modification at Ser^{15} by phosphoinositide 3-kinases, the original characterization of CK1δ specificity in targeting the transactivation domain of p53 showed that mutation of the Ser^{20} site resulted in the most pronounced block of p53 phosphorylation (11).

The function of CK1 in virus signaling was only recently realized, in part, due to the availability of relatively specific inhibitors of CK1. In particular, CK1 was implicated in mediating

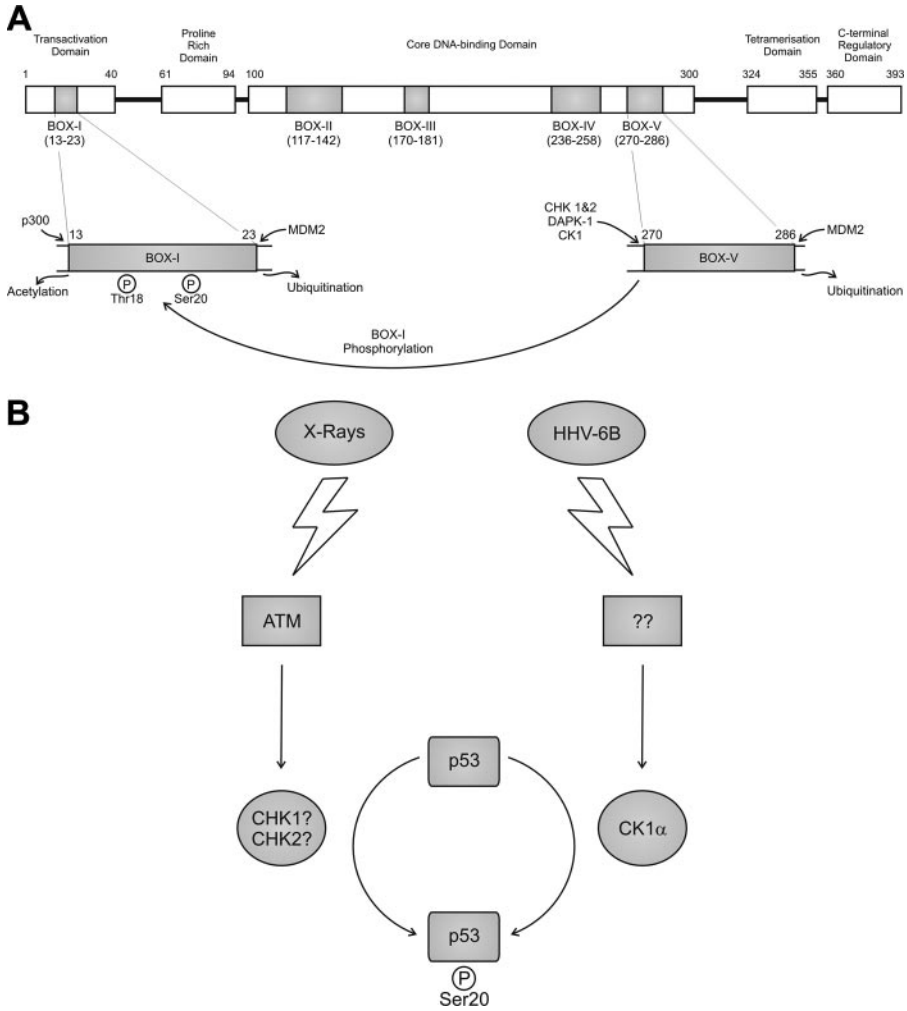

FIGURE 13. **Multiprotein docking site and p53 activation models.** *A*, the interaction of CK1 and calcium calmodulin kinases with the multiprotein docking sites in the *BOX-IV* and *BOX-V* domains of p53 allows their subsequent phosphorylation of Ser^{20} and/or Thr^{18} sites within the *BOX-I* domain of p53. The domain structure of p53 (393 amino acids) is represented, including the conserved domains, labeled with the indicated amino acids flanking *BOX-I* through *BOX-V*. The *BOX-I* domain from amino acid 13 to 23 contains the Thr^{18} and Ser^{20} phosphorylation sites and the N-terminal docking sites for p300 and MDM2 that are required for acetylation and ubiquitination of p53, respectively. The *BOX-V* domain from amino acid 270 to 286 contains the protein kinase and MDM2 docking sites that are required for phosphorylation and ubiquitination, respectively. *B*, different kinase signaling pathways link the two distinct stresses of DNA damage and viral infection to p53 Ser^{20} site phosphorylation and activation. p53 is activated by distinct stresses, including DNA damage, metabolic stress, oncogene activation, and virus infection. CHK1 and/or CHK2 have been implicated as the most likely Ser^{20} site kinases in response to DNA damage (18, 20), but this has been questioned using gene knock-out technologies (21). Thus, the identity of the DNA damage-induced Ser^{20} site kinase is not necessarily evident. By contrast, this current study demonstrates that DNA virus-induced Ser^{20} site phosphorylation of p53 is not mediated by CHK1/2 but rather by CK1. These data support the model that the Ser^{20} site phosphorylation of p53 is triggered by distinct stress-responsive signaling cascades, and future analysis will be required to determine the identity of the enzymes that mediate stress-induced phosphorylation of p53 at this site.

NSP5-dependent rotavirus RNA replication (28) and in mediating hepatitis C virus NS5A protein hyperphosphorylation (29, 30). Whether cells exploit CK1 to modify p53 after infection by RNA viruses or other proapoptotic DNA viruses remains to be established. In addition, whether cells exploit CHK1/2 after virus infection to target p53 remains to be determined; it may be a possibility if DNA replication and genome checkpoints sense and signal to the ataxia telangiectasia-mutated and Rad3-related (ATM/ATR)-CHK1/2 axis. Further, the function of p53 after HHV-6B infection remains to be determined, and the changes in gene expression induced by p53 need to be characterized. Presumably the virus-induced Ser^{20} site phosphorylation will alter p300 binding and related p300 co-activated transcriptional targets. However, we do not know whether this will facilitate virus survival and replication or whether it will facilitate host T-cell responses and organism survival.

Although we identified a novel role for CK1α in linking the p53 checkpoint pathway to the cellular response to DNA virus infection, our studies suggest that distinct kinases are responsible for mediating the phosphorylation of p53 at Ser^{20} after different stresses (model depicted in Fig. 13*B*). For example, Ser^{20} site phosphorylation in response to irradiation damage has been historically attributed to CHK1/2. It therefore appears that distinct stresses lead to the activation of different p53-activating kinases, which presumably enables cells to adopt appropriate stress-specific responses.

In conclusion, the enzymes that coordinately modify p53 protein after cell stress form a relatively large family of enzymes, including kinases, acetyltransferase, and ubiquitin conjugation enzymes. Although irradiation damage has been the most well characterized stress-activating system for p53, in part because anti-cancer agents often function by inducing DNA damage, more physiological stresses have not been as well characterized. In particular, the ability of cells to respond to DNA or RNA virus infection by switching on p53 activation pathways provides an opportunity to identify signaling pathways that might shed light on how viruses target the immune system. In this report, we provide evidence suggesting that CK1 is a major enzyme that targets the transactivation domain of p53 by phosphorylation after HHV-6B infection. Our work highlights CK1 as a component of an intriguing pathway that warrants further investigation in order to understand the interaction between viruses and the mammalian immune system.

REFERENCES

1. Levine, A. J., Hu, W., and Feng, Z. (2006) *Cell Death Differ.* **13,** 1027–1036
2. Hupp, T. R., and Walkinshaw, M. (2007) *Nat. Struct. Mol. Biol.* **14,** 885–887
3. Dornan, D., Shimizu, H., Perkins, N. D., and Hupp, T. R. (2003) *J. Biol. Chem.* **278,** 13431–13441
4. Polley, S., Guha, S., Roy, N. S., Kar, S., Sakaguchi, K., Chuman, Y., Swami-

nathan, V., Kundu, T., and Roy, S. (2008) *J. Mol. Biol.* **376,** 8–12
5. Teufel, D. P., Freund, S. M., Bycroft, M., and Fersht, A. R. (2007) *Proc. Natl. Acad. Sci. U. S. A.* **104,** 7009–7014
6. Hupp, T. R., Sparks, A., and Lane, D. P. (1995) *Cell* **83,** 237–245
7. MacPherson, D., Kim, J., Kim, T., Rhee, B. K., Van Oostrom, C. T., DiTullio, R. A., Venere, M., Halazonetis, T. D., Bronson, R., De Vries, A., Fleming, M., and Jacks, T. (2004) *EMBO J.* **23,** 3689–3699
8. Bruins, W., Zwart, E., Attardi, L. D., Iwakuma, T., Hoogervorst, E. M., Beems, R. B., Miranda, B., van Oostrom, C. T., van den Berg, J., van den Aardweg, G. J., Lozano, G., van Steeg, H., Jacks, T., and de Vries, A. (2004) *Mol. Cell Biol.* **24,** 8884–8894
9. Bruins, W., Jonker, M. J., Bruning, O., Pennings, J. L., Schaap, M. M., Hoogervorst, E. M., van Steeg, H., Breit, T. M., and de Vries, A. (2007) *Carcinogenesis* **28,** 1814–1823
10. Vega, F. M., Sevilla, A., and Lazo, P. A. (2004) *Mol. Cell Biol.* **24,** 10366–10380
11. Dumaz, N., Milne, D. M., and Meek, D. W. (1999) *FEBS Lett.* **463,** 312–316
12. Takaoka, A., Hayakawa, S., Yanai, H., Stoiber, D., Negishi, H., Kikuchi, H., Sasaki, S., Imai, K., Shibue, T., Honda, K., and Taniguchi, T. (2003) *Nature* **424,** 516–523
13. Boutell, C., and Everett, R. D. (2004) *J. Virol.* **78,** 8068–8077
14. Oster, B., Bundgaard, B., and Hollsberg, P. (2005) *J. Virol.* **79,** 1961–1965
15. Oster, B., Bundgaard, B., Hupp, T. R., and Hollsberg, P. (2008) *J. Gen. Virol.* **89,** 87–96
16. Craig, A. L., Bray, S. E., Finlan, L. E., Kernohan, N. M., and Hupp, T. R. (2003) *Methods Mol. Biol.* **234,** 171–202
17. Valbuena, A., Lopez-Sanchez, I., Vega, F. M., Sevilla, A., Sanz-Garcia, M., Blanco, S., and Lazo, P. A. (2007) *Arch. Biochem. Biophys.* **465,** 219–226
18. Craig, A. L., Chrystal, J. A., Fraser, J. A., Sphyris, N., Lin, Y., Harrison, B. J., Scott, M. T., Dornreiter, I., and Hupp, T. R. (2007) *Mol. Cell Biol.* **27,** 3542–3555
19. Craig, A., Scott, M., Burch, L., Smith, G., Ball, K., and Hupp, T. (2003) *EMBO Rep.* **4,** 787–792
20. Shieh, S. Y., Ahn, J., Tamai, K., Taya, Y., and Prives, C. (2000) *Genes Dev.* **14,** 289–300
21. Ahn, J., Urist, M., and Prives, C. (2003) *J. Biol. Chem.* **278,** 20480–20489
22. Wallace, M., Worrall, E., Pettersson, S., Hupp, T. R., and Ball, K. L. (2006) *Mol. Cell* **23,** 251–263
23. Ping-Yuan, L., Hung-Jen, L., Meng-Jiun, L., Feng-Ling, Y., Hsue-Yin, H., Jeng-Woei, L., and Wen-Ling, S. (2006) *Apoptosis* **11,** 2179–2193
24. Sun, Y., and Leaman, D. W. (2005) *J. Biol. Chem.* **280,** 15561–15568
25. Pedersen, S. M., and Hollsberg, P. (2006) *Virology* **356,** 1–3
26. Dornan, D., Shimizu, H., Burch, L., Smith, A. J., and Hupp, T. R. (2003) *Mol. Cell Biol.* **23,** 8846–8861
27. Alsheich-Bartok, O., Haupt, S., Alkalay-Snir, I., Saito, S., Appella, E., and Haupt, Y. (2008) *Oncogene* **27,** 3653–3661
28. Campagna, M., Budini, M., Arnoldi, F., Desselberger, U., Allende, J. E., and Burrone, O. R. (2007) *J. Gen. Virol.* **88,** 2800–2810
29. Quintavalle, M., Sambucini, S., Summa, V., Orsatti, L., Talamo, F., De Francesco, R., and Neddermann, P. (2007) *J. Biol. Chem.* **282,** 5536–5544
30. Quintavalle, M., Sambucini, S., Di Pietro, C., De Francesco, R., and Neddermann, P. (2006) *J. Virol.* **80,** 11305–11312
31. Rena, G, Bain, J., Elliot, M., and Cohen, P. (2004) *EMBO Rep.* **5,** 60–65